Tetrahedron 126 (2022) 133072

Contents lists available at ScienceDirect

Tetrahedron

journal homepage: www.elsevier.com/locate/tet

Discovery of venediols by activation of a silent type I polyketide biosynthetic gene cluster in *Streptomyces venezuelae* ATCC 15439

Shuai Li [a, 1], Lu-Ping Chi [a, 1], Zhong Li [a], Mingyu Liu [a], Ruxin Liu [a], Moli Sang [a], Xianliang Zheng [b], Lei Du [a], Wei Zhang [a], Shengying Li [a, c, *]

[a] State Key Laboratory of Microbial Technology, Shandong University, Qingdao, Shandong, 266237, China
[b] Center for Biocatalysis and Enzyme Technology, AngelYeast Co., Ltd., Yichang, Hubei, 443003, China
[c] Laboratory for Marine Biology and Biotechnology, Qingdao National Laboratory for Marine Science and Technology, Qingdao, Shandong 266237, China

ARTICLE INFO

Article history:
Received 30 August 2022
Received in revised form
28 September 2022
Accepted 1 October 2022
Available online 10 October 2022

Keywords:
Streptomyces venezuelae
Secondary metabolites
Polyketide synthase
Silent biosynthetic gene cluster
CRISPR/Cas9

ABSTRACT

The genus of *Streptomyces* plays an indispensable role in discovery of bioactive secondary metabolites. As a model strain, *Streptomyces venezuelae* ATCC 15439 possesses more than 30 biosynthetic gene clusters (BGCs) in its genome; however, many of which are transcriptionally silent and hence uncharacterized. Here, we apply CRISPR/Cas9 genome editing technology to activate a cryptic type I polyketide biosynthetic gene cluster by site-specific insertion of the constitutive promoter *kasOp**, leading to the discovery of two new polyketide metabolites including venediols A (**1**) and B (**2**). The elucidated structures and heterologous expression of this BGC suggest an unusual loss of colinearity of the modular polyketide synthases during their biosynthesis.

1. Introduction

Streptomyces species are Gram-positive bacteria and excellent cell factories for production of diverse bioactive secondary metabolites, such as antibiotics, parasiticides, antitumor agents, and immunosuppressants [1]. In particular, approximately two-thirds of natural antibiotics are produced by *Streptomyces* [2]. Genome sequencing data have shown that *Streptomyces* spp. contain abundant biosynthetic gene clusters (BGCs) for secondary metabolites. However, a considerable proportion of BGCs are not or low expressed under laboratory culture conditions [3]. Therefore, activation of the silent/cryptic BGCs has become an effective strategy for discovery of novel secondary metabolites [4]. With the development of bioinformatics tools and genome editing technologies, a growing number of efforts have been made to activate silent BGCs, including cloning and expressing cryptic BGCs in heterologous host strains or regulating the expression of these BGCs in native hosts [5,6].

Streptomyces venezuelae ATCC 15439 is a versatile producer of secondary metabolites. This model strain has been extensively studied for the pikromycin biosynthetic system that is responsible for the production of multiple 12- and 14-membered ring macrolide antibiotics (Fig. 1). Recently, this laboratory discovered the diterpene products venezuelaenes A and B by activation of a silent BGC consisting of four biosynthetic genes (*venA–D*) [7]. Moreover, this strain has been used as a heterologous host due to its fast growth rate, simple genetic manipulation, and robust secondary metabolism. With the release of the high-quality whole genome sequences, more than 30 different BGCs were identified from the genome of *S. venezuelae* ATCC 15439, including polyketide, nonribosomal peptide, terpenoid, and other types of secondary metabolites biosynthetic systems [8]. Notably, among many strains classified as *S. venezuelae* species, *S. venezuelae* ATCC 15439 harbors a considerable fraction of strain specific BGCs, exhibiting attractive biosynthetic capacity [9]. To the best of our knowledge, except pikromycin and related macrolides, zincphyrin IV and venezuelaenes [7,10–12] (Fig. 1), the products of other BGCs remain unknown.

To address this issue, we have been paying attention on these unexplored BGCs in order to find more secondary metabolites with new structures and application potentials. Specifically, in this study,

* Corresponding author. State Key Laboratory of Microbial Technology, Shandong University, Qingdao, Shandong, 266237, China.
E-mail address: lishengying@sdu.edu.cn (S. Li).
[1] These authors contributed equally.

https://doi.org/10.1016/j.tet.2022.133072
0040-4020/

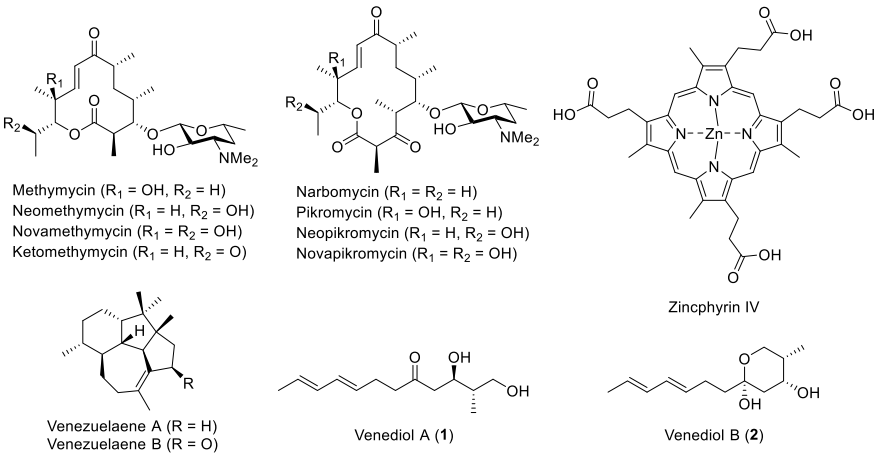

Fig. 1. Structures of secondary metabolites from *S. venezuelae* ATCC 15439.

we report the discovery of two new polyketide compounds including venediols A (**1**) and B (**2**) by the activation of their silent encoding type I polyketide synthase (PKS) BGC.

2. Results and discussion

We first performed a comprehensive analysis of the whole genome of *S. venezuelae* ATCC 15439 (GenBank accession number: CP013129) using the software antiSMASH bacteria version 6.0 [13]. The genome analysis demonstrated that the strain possesses at least 32 BGCs putatively responsible for biosynthesis of polyketides, non-ribosomal peptides, terpenoids, and other secondary metabolites (Table S3). Among these BGCs, a 30 kb BGC (*ved*, Table S4) was revealed to contain three predicted open reading frames (ORFs: *vedA*, *vedB* and *vedC*), presumably encoding three type I PKSs (Fig. 2). This BGC is analogous to the streptazone E BGC of *Streptomyces* sp. MSC090213JE08 [14] (Fig. S1). However, our transcriptomics analysis indicated that the three putative PKS genes were all silent under the tested culture conditions (Table S5). Since the immediately upstream and downstream genes of *vedA*–*C* were transcribed to different substantial extents, we reasoned that the *ved* gene cluster might only contain the three PKS genes.

To investigate the product(s) of *ved*, we elected to activate this BGC *in situ* by incorporating a strong promoter to drive the expression of *vedA*–*C*. Since *S. venezuelae* ATCC 15439 produces a variety of pikromycin-related macrolides (Fig. 1), which may consume significant amounts of PKS precursors as well as building blocks, and complicate the detection of new compounds, we first inactivated the pikromycin biosynthetic pathway by deleting an essential part of the first PKS gene *pikAI* (8,044,206–8,046,225 bp) using the CRISPR/Cas9-based knockout technology. As expected, HPLC analysis of the fermentation extract of the *pikAI*-inactivated strain *Sv*-1 in SCM fermentation medium gave a simplified metabolite profile than that of the wild type strain (*Sv*-WT) by completely losing the ability to produce both 12-membered and 14-membered ring macrolides (Fig. 3).

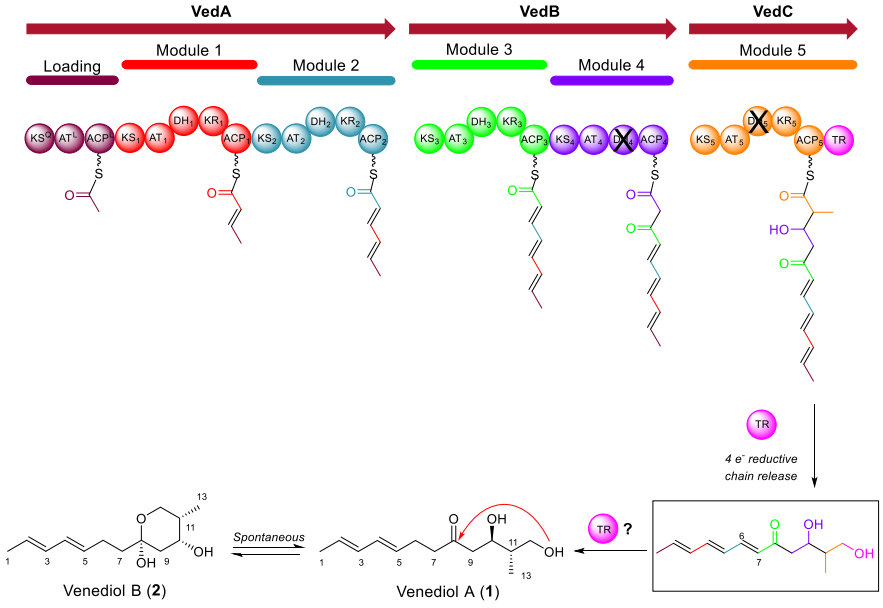

Fig. 2. The proposed biosynthetic pathway of venediols. The modules and domains in the three PKS polypeptides are shown. KS, ketosynthase; KS^Q, KS in which the catalytic Cys is replaced by Gln; AT, acyltransferase; ACP, acyl carrier protein; DH, dehydratase; KR, ketoreductase; TR, thioester reductase.

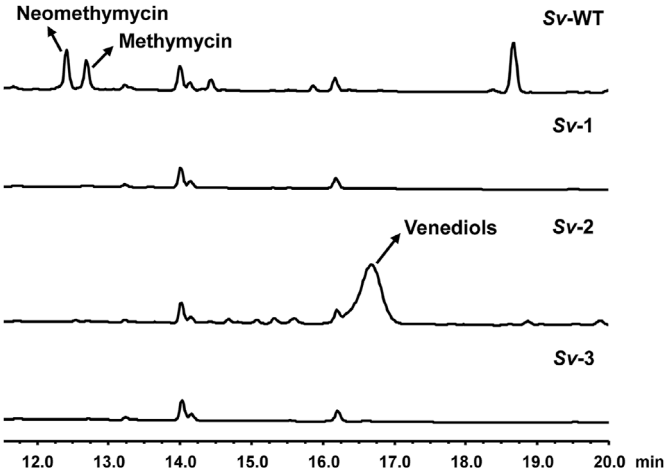

Fig. 3. HPLC analysis (230 nm) of the metabolites produced by the wild type and mutant *S. venezuelae* strains. *Sv*-WT: wild type; *Sv*-1: the *pikAI* inactivated strain; *Sv*-2: the *Sv*-1 strain with the expression of *ved* cluster driven by the promoter *kasO*p*; *Sv*-3: the *Sv*-2 strain with *vedA* inactivated. The peaks corresponding to methymycin and neomethymycin are labeled. The new peak resulted from the activation of *ved* is pointed out by a solid arrow.

Next, we inserted the strong constitutive promoter *kasO*p* [15], which is often used to up-regulate the gene expression in *Streptomyces*, into the upstream of the start codon of *vedA* gene in *Sv*-1, giving rise to the recombinant strain *Sv*-2. As expected, HPLC analysis of the fermentation extract of *Sv*-2 showed a new peak with the maximum absorption peak at 227 nm (Fig. 3). To confirm this new peak was resulted from the activation of *ved* cluster, we deleted a 2,020 bp fragment of *vedA* in *Sv*-2 to interrupt this biosynthetic system. As a result, the metabolic profile of the *vedA*-inactivated mutant *Sv*-3 changed back to that of *Sv*-WT (Fig. 3), clearly indicating that *ved* was successfully activated upon promoter engineering.

To isolate the *ved*-related product, *Sv*-2 was cultured in SCM medium for 7 d in shaking flasks at 30 °C. The new product peak was purified from the organic extract of the *Sv*-2 culture broth by preparative C18 reversed-phase HPLC. The molecular formula was assigned to be $C_{13}H_{22}O_3$ based on HR-ESI-MS analysis, which gave a pseudomolecular ion $[M+Na]^+$ peak at *m*/*z* 249.1467, suggesting three degrees of unsaturation. However, the ^1H and ^{13}C NMR spectra (Table 1) showed the presence of four methyl groups, eight sp^3 hybridized methylenes (with two oxygenated), eight sp^2 hybridized methines and four sp^3 hybridized methines (including two bonded to oxygen), one sp^2 hybridized non-protonated carbonyl carbon, and one sp^3 hybridized non-protonated oxygenated carbon. Careful analysis of 1D and 2D NMR spectra revealed its nature of an inseparable mixture, consisting of two components **1** and **2**. The COSY correlations showed the spin systems from H-1 to H-7 and from H-9 to H-12 via H-13 in **1** and **2**. For compound **1**, the two fragments were connected by the HMBC correlations from H-6, H-7, H-9 and H-10 to C-8. Meanwhile, HMBC correlations from H-6, H-7, H-9, H-10 and H-12 to C-8 confirmed the proposed structure of **2** (Fig. 4). Of note, compound **1** with a keto group showed a tendency to form an intramolecular hemiacetal to give **2**. According to the structural features and biological origin, we named **1** and **2** as venediols A and B, respectively.

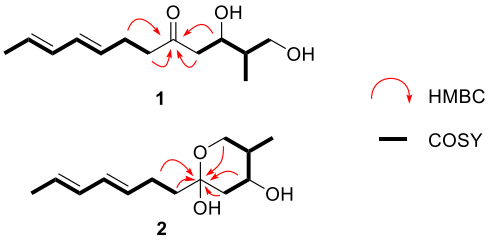

Fig. 4. COSY and key HMBC correlations of venediols **1** and **2**.

To establish the relative configurations of **1**, *J*-based configurational analysis (JBCA) was conducted. The large coupling constant of H-10 and H-11 ($^3J_{H\text{-}10,H\text{-}11} = 7.9$ Hz) revealed an *anti* arrangement of the two protons in Newman projection, and NOE cross-peaks from H-9 and H-10 to H-13 established the *erythro* configuration of C-10 and C-11 in Fisher projection, which allowed the relative configurations of C-10 and C-11 to be assigned as 10*R** and 11*S** (Fig. S9). To further confirm the relative configurations of the stereogenic centers C-10 and C-11, both proton and carbon data of two possible isomers (**1a** and **1b**, Fig. S10) were calculated based on the DP4+ protocol [16]. The statistical comparison of the calculated data with experimental values indicated that the isomer **1b** was the equivalent structure with a probability of 100%, which is consistent with the JBCA results. The relative configurations of **2** were similarly assigned to be 8*R**, 10*R** and 11*S** by DP4+ probability analysis, on account of the experimental NMR data matching well (100%) with those calculated for the isomer **2b** (Fig. S10).

Furthermore, the absolute configurations of **1** and **2** were deduced through bioinformatics analysis of the ketoreductase (KR)

Table 1
NMR data for venediols A (**1**) and B (**2**) in $CDCl_3$ (^1H at 600 MHz,^{13}C at 150 MHz).

Position	1		2	
	δ_C, type	δ_H (*J* in Hz)	δ_C, type	δ_H (*J* in Hz)
1	18.2, CH_3	1.74, d (6.1)	18.2, CH_3	1.74, d (6.1)
2	127.5, CH	5.59, overlapped	128.2, CH	5.59, overlapped
3	131.6, CH	6.01, overlapped	131.3, CH	6.01, overlapped
4	131.7, CH	6.01, overlapped	130.9, CH	6.01, overlapped
5	129.2, CH	5.49, dd (14.2, 7.2)	131.3, CH	5.55, overlapped
6	26.6, CH_2	2.34, q (7.2)	26.3, CH_2	2.21, m
7	43.4, CH_2	2.54, t (7.2)	41.8, CH_2	1.67, dd (7.2, 4.9)
8	211.8, C		97.4, C	
9	47.4, CH_2	2.70, dd (17.6, 2.3)	39.2, CH_2	2.02, dd (14.1, 3.1)
		2.57, dd (17.6, 9.8)		1.69, dd (14.1, 3.1)
10	73.4, CH	4.00, ddd (9.8, 7.9, 2.3)	69.1, CH	3.94, s
11	39.8, CH	1.75, m	34.5, CH	1.82, ddd (11.8, 7.0, 5.0)
12	67.6, CH_2	3.66, m	61.4, CH_2	3.81, d (11.8)
				3.48, dd (11.8, 5.0)
13	13.2, CH_3	0.87, d (7.0)	13.8, CH_3	0.90, d (7.0)

domains in venediol PKSs. The multiple protein alignment showed that all KR domains (KR1, KR2, KR3 and KR5) contain the typical "LDD" motif, thus being classified as the B-type KRs, which presumably generate the hydroxy groups of *R* configuration (Fig. 5C) [17,18]. This analysis strongly suggests that the C-10 hydroxyl group of venediols should adopt the *R* configuration. Taken together, the absolute configurations of **1** and **2** were determined as 10*R*,11*S* and 8*R*,10*R*,11*S*, respectively.

With regard to venediol biosynthesis, we analyzed a total of 28 enzymatic domains organized into six modules (Fig. 2). The smallest loading module contains acyltransferase (AT), ketosynthase (KS^Q), and acyl carrier protein (ACP) domains, in which the catalytic cysteine residue of a normal KS is replaced by a glutamine, giving rise to a KS^Q domain to decarboxylate malonate forming an acetyl group as the starting unit of the polyketide chain assembly (Fig. 5A) [19]. The same KS^Q domain has been found in many type I PKS systems, such as pikromycin [20] and lavendiol [21]. All remaining KS domains (KS1–5) appear to be active as they each have a full set of catalytic residues responsible for decarboxylative condensation. The AT domain of module 5 (AT5) contains GHSQG and YASH motifs that specifically transfer methylmalonyl moiety, whereas all other extender AT domains having GHS(I/V)G and HAFH motifs are specific for malonyl moieties (Fig. 5B) [22,23]. The predicted linear assembly of these malonyl and methymalonyl building blocks is consistent with the backbone structure of venediols. Before the next extension step, the β-ketoacyl moiety tethered to the phosphopantetheinyl arm of ACP domain is supposed to be alternatively modified by KR, DH and ER, which set complexity and stereochemistry of diverse polyketides. Interestingly, ER is completely absent in venediol biosynthesis. Sequence analysis

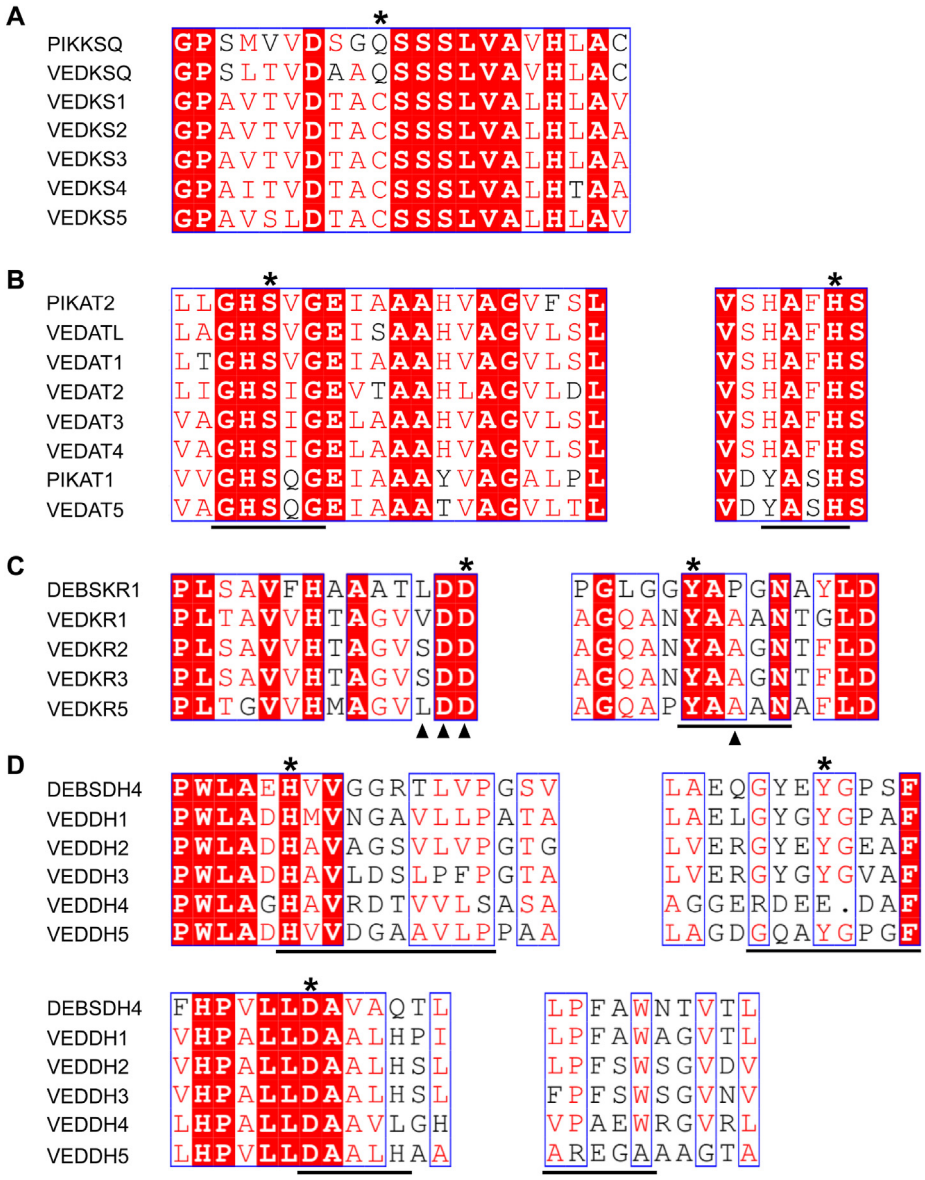

Fig. 5. Protein sequence alignments of KS (A), AT (B), KR (C), DH (D) domains from venediol PKSs with the selected representative functional domains. The PKS names and sequence accession numbers are as follows: VED, venediol, Table S4; PIK, pikromycin, AF079138; DEBS, erythromycin, L07626. (A) The asterisk indicates the conserved catalytic residue; KS^Q, in which the active-site cysteine residue is replaced by glutamine. (B) The conserved sequence motifs used to select extender units are underlined. Asterisks indicate the conserved catalytic residues. (C) Solid triangles denote the consensus motifs for B1-type KR (LDD, no P). The conserved sequence motif YAAAN is underlined. The conserved aspartic acid residues of LDD motif and the catalytic tyrosine are indicated by asterisks. (D) Important conserved sequence motifs, including HXXXGXXXXP, GYXYGPXF, DXXX(Q/H) and LPFXW, are underlined. The catalytic histidine, tyrosine and aspartic acid are marked by asterisks.

revealed that all KR domains (KR1, KR2, KR3 and KR5) belong to B1-type and should yield a hydroxy group of *R* configuration (Fig. 5C) [17].

The DH domain catalyzes the dehydration of β-hydroxyl group resulting from the stereoselective reduction by the KR domain to yield a *trans* double bond. Consistently, all the double bonds in venediols adopt a *trans* configuration. Regarding the venediol DH domains, the functional DH domains (DH1 and DH2) possess the signature HXXXGXXXXP motif and other conserved motifs (Fig. 5D). By contrast, the DH domains of module 4 (DH4) and 5 (DH5) are likely nonfunctional since both domains contain significant alterations to the LPFXW motif as the inactive DH6 and DH7 domains involved in rifamycin biosynthesis [24]. In addition, DH4 of VedB lacks the conserved GYXYGPXF motif, further supporting its inactivity. This is unsurprising because an adjacent KR domain is absent in module 4, thus making a DH domain useless. The non-functionality of DH5 is consistent with the presence of the C-10 hydroxy group in products. With regard to DH3, despite it contains an FPFSW (rather than the consensus sequence LPFXW) motif, we still speculate that DH3 should be a functional domain since the homologous functional DH3 domain involved in streptazone E biosynthesis possesses a similar Leu-to-Val mutation in the LPFXW motif.

Intriguingly, the presence of the C-6/C-7 single bond in both **1** and **2** is totally unexpected in the absence of an ER domain. Specifically, due to the dehydration activity of DH3, a C-6/C-7 double bond is supposed to be formed in products. Thus, there must be an additional gene product responsible for the reduction of the C6/C7 double bond. To determine whether this gene is inside or outside the *ved* cluster, we directly cloned the whole gene cluster using Red/ET technology [25] and heterologously expressed VedA–C in *Streptomyces coelicolor* M1152 [26]. As a result, VedA–C still produced **1** and **2** (Figs. S11 and S12), strongly suggesting that the gene responsible for the C6/C7 saturation is within the *ved* cluster. Possibly, the TR domain with reductase functionality might be able to reduce the C6/C7 double bond with an unusual mechanism (Fig. 2). However, although unlikely, we cannot rule out the possibility that some homologous reductases in primary metabolism, shared by *S. venezuelae* and *S. coelicolor* might be responsible for reducing the C6/C7 double bond.

Finally, we found that a normal thioesterase (TE) domain responsible for termination of polyketide assembly is absent in VedC. Instead, a thioester reductase (TR) domain is embedded in module 5, which is homologous (70%/81% identity/similarity) to that of CpkC in the biosynthesis of coelimycin P1 [27]. It is well known that the aldehyde intermediate generated by TR domain is unstable and need to be further reduced to alcohol or undergo other modifications [28]. Thus, we speculate that the TR domain of VedC might catalyze both the C6/C7 saturation as described above and the NAD(P)H-dependent four-electron reductive release of the hexaketide **1** [28]. Since **1** has the C-8 ketone and C-12 hydroxyl group, which tends to intramolecularly form a 6-membered ring hemiacetal to give **2**, similar to gephyronic acid [29].

3. Conclusion

Extensive genomic sequencing has revealed that *Streptomyces* spp. carry a large number of secondary metabolite BGCs. However, a majority of these BGCs are silent or marginally expressed under laboratory culture conditions. In the synthetic biology era, activation of silent or weak BGCs is an important strategy for discovering new compounds to combat the growing prevalence of antibiotic resistances. We previously explored the cryptic terpenoid BGC through a genome mining approach and discovered two new compounds venezuelaenes A and B by silent gene activation [7]. Together with venediols A and B discovered in this study, these hidden metabolites indicate that *S. venezuelae* ATCC 15439 has the potential for discovery of more novel secondary metabolites.

In summary, the discovery of venediols increases the diversity of *Streptomyces* secondary metabolites. In the future, we need to find an effective way to separate **1** and **2** in order to test their biological activities individually. The loss of colinearity of the type I modular PKS of venediols raise a key question on how the C6/C7 double bond is reduced without an ER domain. Since the venediol biosynthesis has no any post-tailoring steps, we putatively proposed that the unexpected C-6/C-7 saturation might be mediated by the final TR domain. Further genetic and biochemical studies are required to elucidate the exact biogenetic mechanism, which is currently ongoing in our laboratory. Of note, the *in situ* activation of *ved* BGC did not result in any downstream products, suggesting that the *ved* gene cluster might only have three PKS genes. Nonetheless, it is too early to exclude the possibility that some post-tailoring genes located at the upstream or downstream of *ved* might be silent since we have not fully activated these genes yet. Thus, it is intriguing to further investigate these potential post-PKS tailoring enzymes as those involved in streptazone E biosynthesis [14].

4. Experimental

4.1. Strains, plasmids, media, and culture conditions

All bacterial strains and plasmids used in this study are listed in Supplementary data, Table S1. *Escherichia coli* strains were cultured at 37 °C on LB agar or in LB liquid media. *Streptomyces venezuelae* ATCC 15439 (a gift from Prof. Yeo Joon Yoon at Seoul National University), *Streptomyces coelicolor* M1152 (a gift from Prof. Jianhua Ju at Shandong University), and their derivatives were grown at 30 °C on mannitol soya flour (MS) agar (20 g soy flour, 20 g mannitol, 20 g agar per liter) for sporulation and conjugation. 2 × YT (16 g tryptone, 10 g yeast extract, and 5 g NaCl per liter) liquid media were used to grow seed cultures for *Streptomyces* strains. SCM (15 g soluble starch, 20 g soytone, 0.1 g $CaCl_2$, 1.5 g yeast extract and 10.5 g MOPS per liter, pH 7.2) media were used as the secondary metabolites production media for *Streptomyces* strains. Liquid cultures were shaken in 30 ml of media in 250 ml flasks. MS media supplemented with 50 mM $MgCl_2$ and 50 mM $CaCl_2$ were used for intergeneric conjugation between *E. coli* and *Streptomyces* [30]. Antibiotics were supplemented at the following concentrations when required: 25 μg ml^{-1} chloramphenicol, 50 μg ml^{-1} kanamycin, 50 μg ml^{-1} apramycin, and 25 μg ml^{-1} nalidixic acid.

4.2. Materials

All restriction enzymes were purchased from Thermo Scientific (Waltham, USA) and Takara (Dalian, China). The chemicals and antibiotics used in this study were bought from Solarbio (Beijing, China), Sinopharm Chemical Reagent (Beijing, China), and Sangon (Shanghai, China) unless otherwise specified. ClonExpress Ultra One Step Cloning Kit was obtained from Vazyme (Nanjing, China). PrimeSTAR Max DNA Polymerase (Dalian, China) was employed to amplify DNA fragments by PCR reactions. T4 DNA polymerase was purchased from New England Biolaboratory (Beijing, China).

4.3. DNA sequencing and bioinformatics analysis

Primers were synthesized by Sangong (Qingdao, China). DNA sequencing was performed by TsingKe (Qingdao, China). Gene annotations and functional predictions of the biosynthetic gene cluster were carried out using NCBI databases and antiSMASH

bacterial version (https://secondarymetabolites.org/) [13]. Protein sequence alignment was performed using ClustalW and the results were output by ESPript 3.0 [31]. DNA sequence alignment was conducted using DNAman 7.0. Transcriptome data were disclosed in our previous work [7].

4.4. Construction of the gene knock-out and knock-in plasmids

All the primers used for plasmid construction and clone screening are listed in Supplementary data, Table S2. Both the gene knock-out plasmids and the *kasO*p* knock-in plasmid were derived from the modifications of the CRISPR/Cas9 genome editing plasmid pKCcas9dO [32]. To generate the *pikAI* (5621010–5623029 bp) deletion plasmid pKCcas9dP, the *pikAI* deletion sgRNA expressing cassette was amplified from pKCcas9dO with the primers PikAIgRNA-F and PikAIgRNA-R. Two homologous arms flanking *pikAI* were amplified from *S. venezuelae* genomic DNA separately with the primer pairs PikAILA-F/PikAILA-F and PikAIRA-F/PikAIRA-R. Similarly, to generate the plasmid pKCcas9dVA for *vedA* (8044206–8046225 bp) deletion, the *vedA* deletion sgRNA expressing cassette was amplified from pKCcas9dO with the primers VedAgRNA-F and VedAgRNA-R. Two homologous arms flanking *vedA* (8044206–8046225 bp) were amplified from *S. venezuelae* genomic DNA separately with the primer pairs VedALA-F/VedALA-F and VedARA-F/VedARA-R. To construct the *kasO*p* knock-in plasmid pKCcas9dOVK, the *kasO*p* insertion sgRNA expressing cassette was amplified from pKCcas9dO with the primers VedKRNA-F and VedKgRNA-R. Two homologous arms containing the *kasO*p* promoter sequence were amplified from *S. venezuelae* genomic DNA separately with the primer pairs VedKLA-F/VedKLA-R and VedKRA-F/VedKRA-R. The above three amplicons for each individual plasmids were ligated to the *Spe*I/*Hind*III linearized pKCcas9dO vector with ClonExpress Ultra One Step Cloning Kit. Correct plasmid assemblies were confirmed by DNA sequencing, and the plasmids were subsequently used to transform *S. venezuelae* strains.

4.5. Construction of the plasmid carrying the vedA-C genes

For heterologous expression of *vedA-C* in *S. coelicolor* M1152, the *ved* cluster was directly cloned and genetically engineered by Red/ET recombineering [33]. Genomic DNA of *S. venezuelae* was digested with *Mau*BI to release the 48 kb *ved* gene cluster. Using p15A-cm-ved1/2 as PCR primers containing homology arms flanking *ved*, and using the cloning vector p15A-cm-tetR-tetO-hyg-ccdB as the template, the linear vector p15A-cm was obtained by PCR amplification. The digested genomic DNA and the homology-arm-flanked linear vector were assembled with T4 DNA polymerase *in vitro*. Subsequently, the assembly products were desalted at room temperature, and co-electroporated into *E. coli* GB05-dir to give the vector p15A-cm-ved. The correct transformants were screened on the LB agar plate containing chloramphenicol, and the p15A-cm-ved vectors were further validated by *Bam*HI digestion (Fig. S13). Furthermore, using p15A-apra-*kasO*p*-phiC31 as the template and p15-Apra-*kasO*p*-1/2 as the primers containing the homology arms flanking *ved*, PCR amplification was performed to obtain the product p15-Apra-*kasO*p* carrying the homology arms of the genes flanking *ved*. Then, the fragment p15-Apra-*kasO*p* and p15A-cm-ved plasmid were co-electroporated into *E. coli* GB08-red to obtain the vector p15-Apra-*kasO*p*-ved. The p15-Apra-*kasO*p*-ved vectors prepared from the transformants grown on LB agar containing apramycin were verified by *Bam*HI digestion (Fig. S13).

4.6. Construction and fermentation of recombinant streptomyces strains

Gene knock-out and knock-in plasmids constructed by CRISPR/Cas9 technology and the *ved* heterologous expression plasmids were transferred via interspecies conjugation from *E. coli* ET12567/pUZ8002 to *S. venezuelae* or *S. coelicolor* M1152 by following the standard *Streptomyces* protocols [30]. Briefly, after incubation for 14–16 h at 30 °C, the MS plates were covered with nalidixic acid and apramycin, and incubated until exconjugants appeared. Exconjugants were streaked onto MS plates containing apramycin for genetic confirmation by PCR and DNA sequencing (Fig. S14). Subsequently, correct *S. venezuelae* recombinant strains were cultured at 37 °C to lose the CRISPR/Cas9 plasmid *in vivo*. The *ved* cluster was inserted into the *S. coelicolor* M1152 genome by PhiC31 integrase in the plasmid p15A-phiC31-*kasO*p*-ved, and the screening of *S. coelicolor* recombinant strains was carried out by HPLC and LC-MS analyses of fermentation extracts. For PCR confirmation of *Sv*-1, *Sv*-2 and *Sv*-3, the primers were PikAIYZ-F/PikAIYZ-R, VedKYZ-F/VedKYZ-R, and VedAYZ-F/VedAYZ-R; and the expected lengths of PCR products were 963, 1087 and 1072 bp, respectively (Fig. S14). As for the fermentation of recombinant *S. venezuelae* and *S. coelicolor* strains, a single colony of specific strains was grown on MS agar for 4 d, and inoculated into 2 × YT medium at 30 °C with constant shaking at 220 rpm for 36 h, and then the seed culture was inoculated into SCM with a ratio of 1:10 at 30 °C with constant shaking at 220 rpm for 7 d. The culture broth of each strain was extracted twice with an equal volume of ethyl acetate. The extract was evaporated *in vacuo* and the N_2-dried extract was re-dissolved in 1 ml of methanol. The metabolites from *Streptomyces* strains were monitored by HPLC and LC-MS analyses.

4.7. Isolation and characterization of venediols

All HPLC analyses of crude extract were performed using a reversed phase YMC Triart C-18 column (4.6 mm × 250 mm, 5 μm) on a Thermo UltiMate 3000 instrument with a mobile phase of water and acetonitrile both containing 0.1% trifluoroacetic acid at the flow rate of 1 ml/min. A linear gradient program of acetonitrile in water (10% for 0–1 min, 10–100% for 2–26 min, 100% for 26–30 min, and 10% for 31–33 min) was used for chromatography. The monitoring wavelength was set at 230 nm. HR-LCMS was performed on a Bruker Maxis UHR-TOF equipment. NMR spectra were recorded on a Bruker Avance III 600 MHz spectrometer, using the solvent chemical shifts ($CDCl_3$: δ_H/δ_C 7.26/77.16) as reference. To isolate and identify the structure of venediols, crude extract was further purified by semi-preparative HPLC on a reversed phase YMC Pack Pro C-18 column (10 mm × 250 mm, 5 μm) on a Thermo UltiMate 3000 instrument with a linear gradient system of acetonitrile in water (10% for 0–1 min, 10–100% for 2–26 min, 100% for 26–30 min, and 10% for 31–33 min) at a flow rate of 2.5 ml/min and the wavelength of 230 nm, yielding the inseparable mixture of **1** and **2**: colorless oil; UV (MeOH) λ_{max} (log ε) 227 (3.69) nm; ^{1}H and ^{13}C NMR data, Table 1; HRESIMS *m/z* 249.1467 $[M + Na]^+$ (*calc.* for $C_{13}H_{22}O_3Na$, 249.1467), 475.3035 $[2\,M + Na]^+$ (*calc.* for $C_{26}H_{44}O_6Na$, 475.3036).

4.8. Computational NMR chemical shift calculation and DP4+ analyses

First, conformational searches for possible isomers were conducted through molecular mechanics using the MMFF method with Macromodel software (Schrödinger, LLC) to collect the

corresponding stable conformers. After that, the conformers were optimized at B3LYP/6-31G(d) PCM level. Then, their NMR shielding tensors were calculated using the DFT method at mPW1PW91\6-31 + G(d) PCM level and averaged based on Boltzmann distribution theory [16]. Finally, the NMR chemical shifts and shielding tensors (both ^{1}H and ^{13}C) were analyzed and compared with experimental chemical shifts using DP4+ probability [34].

Declaration of competing interest

The authors declare that they have no known competing financial interests or personal relationships that could have appeared to influence the work reported in this paper.

Data availability

Data will be made available on request.

Acknowledgements

This work was financial supported by the National Key Research and Development Program of China (2019YFA0905100), National Natural Science Foundation of China (32025001 and 32170088), the Shandong Provincial Natural Science Foundation (ZR2019ZD20), and the China Postdoctoral Science Foundation (2021M701989). We thank Prof. Yinhua Lu at Shanghai Normal University and Prof. Youming Zhang at Shandong University for providing us with necessary plasmids and protocols.

Appendix A. Supplementary data

Supplementary data to this article can be found online at https://doi.org/10.1016/j.tet.2022.133072.

References

[1] Y. Ohnishi, J. Ishikawa, H. Hara, H. Suzuki, M. Ikenoya, H. Ikeda, A. Yamashita, M. Hattori, S. Horinouchi, J. Bacteriol. 190 (11) (2008) 4050–4060.
[2] Z. Liu, Y. Zhao, C. Huang, Y. Luo, Front. Bioeng. Biotechnol. 9 (2021), 632230.
[3] D. Mao, B.K. Okada, Y. Wu, F. Xu, M.R. Seyedsayamdost, Curr. Opin. Microbiol. 45 (2018) 156–163.
[4] P.J. Rutledge, G.L. Challis, Nat. Rev. Microbiol. 13 (8) (2015) 509–523.
[5] M. Zhang, F. Wong, Y. Wang, S. Luo, Y.H. Lim, E. Heng, W.L. Yeo, R.E. Cobb, B. Enghiad, E.L. Ang, H. Zhao, Nat. Chem. Biol. 13 (6) (2017) 607–609.
[6] R.H. Baltz, J. Ind. Microbiol. Biotechnol. 37 (8) (2010) 759–772.
[7] Z. Li, Y. Jiang, X. Zhang, Y. Chang, S. Li, X. Zhang, S. Zheng, C. Geng, P. Men, L. Ma, Y. Yang, Z. Gao, Y. Tang, S. Li, ACS Catal. 10 (10) (2020) 5846–5851.
[8] J.Y. Song, Y.J. Yoo, S.K. Lim, S.H. Cha, J.E. Kim, J.H. Roe, J.F. Kim, Y.J. Yoon, J. Biotechnol. 219 (2016) 57–58.
[9] W. Kim, N. Lee, S. Hwang, Y. Lee, J. Kim, S. Cho, B. Palsson, B.K. Cho, Biomolecules 10 (6) (2020) 864–881.
[10] S.K. Lee, J.W. Park, J.W. Kim, W.S. Jung, S.R. Park, C.Y. Choi, E.S. Kim, B.S. Kim, J.S. Ahn, D.H. Sherman, Y.J. Yoon, J. Nat. Prod. 69 (5) (2006) 847–849.
[11] Q. Zhang, D.H. Sherman, J. Nat. Prod. 64 (11) (2001) 1447–1450.
[12] H.T. Nguyen, V.T.T. Pham, C.T. Nguyen, A.R. Pokhrel, T.S. Kim, D. Kim, K. Na, T. Yamaguchi, J.K. Sohng, Appl. Microbiol. Biotechnol. 104 (2) (2020) 713–724.
[13] K. Blin, S. Shaw, A.M. Kloosterma, Z. Charlop-Powers, G.P. Wezel, M.H. Medema, T. Weber, Nucleic Acids Res. 49 (W1) (2021) W29–W35.
[14] S. Ohno, Y. Katsuyama, Y. Tajima, M. Izumikawa, M. Takagi, M. Fujie, N. Satoh, K. Shin-Ya, Y. Ohnishi, Chembiochem 16 (16) (2015) 2385–2391.
[15] W. Wang, X. Li, J. Wang, S. Xiang, X. Feng, K. Yang, Appl. Environ. Microbiol. 79 (14) (2013) 4484–4492.
[16] N. Grimblat, M.M. Zanardi, A.M. Sarotti, J. Org. Chem. 80 (24) (2015) 12526–12534.
[17] P. Caffrey, Chembiochem 4 (7) (2003) 654–657.
[18] X. Zhang, Z. Li, L. Du, G.E. Chlipala, P.C. Lopez, W. Zhang, D.H. Sherman, S. Li, Tetrahedron Lett. 57 (52) (2016) 5919–5923.
[19] A. Witkowski, A.K. Joshi, Y. Lindqvist, S. Smith, Biochemistry 38 (36) (1999) 11643–11650.
[20] Y. Xue, D. Wilson, D.H. Sherman, Gene 245 (1) (2000) 203–211.
[21] I.G.U. Pait, S. Kitani, F.W. Roslan, D. Ulanova, M. Arai, H. Ikeda, T. Nihira, J. Ind. Microbiol. Biot. 45 (2) (2018) 77–87.
[22] W. Zhang, J.L. Fortman, J.C. Carlson, J. Yan, Y. Liu, F. Bai, W. Guan, J. Jia, T. Matainaho, D.H. Sherman, S. Li, Chembiochem 14 (3) (2013) 301–306.
[23] A.T. Keatinge-Clay, Nat. Prod. Rep. 29 (10) (2012) 1050–1073.
[24] P.R. August, L. Tang, Y.J. Yoon, S. Ning, R. Müller, T.W. Yu, M. Taylor, D. Hoffmann, C.G. Kim, X. Zhang, C.R. Hutchinson, H.G. Floss, Chem. Biol. 5 (2) (1998) 69–79.
[25] H. Wang, Z. Li, R. Jia, Y. Hou, J. Yin, X. Bian, A. Li, R. Müller, A.F. Stewart, J. Fu, Y. Zhang, Nat. Protoc. 11 (7) (2016) 1175–1190.
[26] J.P. Gomez-Escribano, M.J. Bibb, Microb. Biotechnol. 4 (2) (2011) 207–215.
[27] J.P. Gomez-Escribano, L. Song, D.J. Fox, V. Yeo, M.J. Bibb, G.L. Challis, Chem. Sci. 3 (9) (2012) 2716–2720.
[28] M.W. Mullowney, R.A. McClure, M.T. Robey, N.L. Kelleher, R.J. Thomson, Nat. Prod. Rep. 35 (9) (2018) 847–878.
[29] J. Young, D.C. Stevens, R. Carmichael, J. Tan, S. Rachid, C.N. Boddy, R. Müller, R.E. Taylor, J. Nat. Prod. 76 (12) (2013) 2269–2276.
[30] T. Kieser, M.J. Bibb, M.J. Butter, K.F. Chater, D.A. Hopwood, Practical Streptomyces Genetics, vol. 291, John Innes Foundation Norwich, 2000, p. 613.
[31] X. Robert, P. Gouet, Nucleic Acids Res. 42 (Web Server issue) (2014) W320–W324.
[32] H. Huang, G. Zheng, W. Jiang, H. Hu, Y. Lu, Acta Biochim. Biophys. Sin. 47 (4) (2015) 231–243.
[33] H. Wang, Z. Li, R. Jia, J. Yin, A. Li, L. Xia, Y. Yin, R. Müller, J. Fu, A.F. Stewart, Y. Zhang, Nucleic Acids Res. 46 (5) (2018) e28.
[34] S.R. Lee, D. Lee, M. Park, J.C. Lee, H.J. Park, K.S. Kang, C.E. Kim, C. Beemelmanns, K.H. Kim, J. Nat. Prod. 83 (2020) 354–361.